

# Lawrence Berkeley National Laboratory

## LBL Publications

### Title

Newly Commissioned iP2 Beamline of the BELLA PW Facility for Investigation of High Intensity Laser-Solid Interactions

### Permalink

<https://escholarship.org/uc/item/6mn265qg>

### Authors

Hakimi, Sahel  
Obst-Huebl, Lieselotte  
Nakamura, Kei  
[et al.](#)

### Publication Date

2022-11-11

### DOI

10.1109/aac55212.2022.10822936

Peer reviewed

# Newly commissioned iP2 beamline of the BELLA PW facility for investigation of high intensity laser-solid interactions

1<sup>st</sup> Sahel Hakimi

*Lawrence Berkeley National Laboratory*  
Berkeley, California 94720, USA  
sahelh@lbl.gov

2<sup>nd</sup> Lieselotte Obst-Huebl

*Lawrence Berkeley National Laboratory*  
Berkeley, California 94720, USA  
lobsthuebl@lbl.gov

3<sup>rd</sup> Kei Nakamura

*Lawrence Berkeley National Laboratory*  
Berkeley, California 94720, USA  
knakamura@lbl.gov

4<sup>th</sup> Axel Huebl

*Lawrence Berkeley National Laboratory*  
Berkeley, California 94720, USA  
axelhuebl@lbl.gov

5<sup>th</sup> Stepan S. Bulanov

*Lawrence Berkeley National Laboratory*  
Berkeley, California 94720, USA  
sbulanov@lbl.gov

6<sup>th</sup> Anya Jewell

*Lawrence Berkeley National Laboratory*  
Berkeley, California 94720, USA  
ajewell@lbl.gov

7<sup>th</sup> Jared T. De Chant

*Lawrence Berkeley National Laboratory*  
Berkeley, California 94720, USA  
jtdechant@lbl.gov

8<sup>th</sup> Antoine M. Snijders

*Lawrence Berkeley National Laboratory*  
Berkeley, California 94720, USA  
amsnijders@lbl.gov

9<sup>th</sup> Csaba Toth

*Lawrence Berkeley National Laboratory*  
Berkeley, California 94720, USA  
ctoth@lbl.gov

10<sup>th</sup> Anthony J. Gonsalves

*Lawrence Berkeley National Laboratory*  
Berkeley, California 94720, USA  
ajgonsalves@lbl.gov

11<sup>th</sup> Carl B. Schroeder

*Lawrence Berkeley National Laboratory*  
Berkeley, California 94720, USA  
CBSchroeder@lbl.gov

12<sup>th</sup> Jeroen van Tilborg

*Lawrence Berkeley National Laboratory*  
Berkeley, California 94720, USA  
jvantilborg@lbl.gov

13<sup>th</sup> Jean-Luc Vay

*Lawrence Berkeley National Laboratory*  
Berkeley, California 94720, USA  
jlway@lbl.gov

14<sup>th</sup> Eric Esarey

*Lawrence Berkeley National Laboratory*  
Berkeley, California 94720, USA  
ehesarey@lbl.gov

15<sup>th</sup> Cameron G. R. Geddes

*Lawrence Berkeley National Laboratory*  
Berkeley, California 94720, USA  
crgeddes@lbl.gov

**Abstract**—The newly commissioned short focal length, high intensity beamline, named iP2, at the BELLA Center enables frontier experiments in high energy density science. This 1 Hz system provides a focused beam of  $<3$  micron in FWHM, resulting in an on-target peak intensity greater than  $5 \times 10^{21}$  W/cm<sup>2</sup>, and a pointing fluctuation on the order of 1  $\mu$ rad. A temporal contrast ratio of  $<10^{-14}$  on the nanosecond timescale is expected with the addition of an on-demand double plasma mirror setup in the near future. This beamline is well suited for studies requiring ultra-high intensity and substantial control over the temporal contrast, such as investigation of novel regimes of

advanced ion acceleration and their applications. The recent results from iP2 high power commissioning experiments are presented as well as the outlook for *in vivo* radiobiological studies at ultra-high dose rates. In preparation for an experimental campaign to investigate the magnetic vortex acceleration regime, a series of 3D simulations using the WarpX code were performed to optimize the target design and guide the development of the main diagnostics. We studied the acceleration performance with different laser temporal contrast conditions at normal and oblique laser incidence angles.

**Index Terms**—High intensity laser systems, Laser-plasma interactions, Laser-driven ion acceleration, Advanced ion acceleration mechanisms, Magnetic Vortex Acceleration regime, Particle-in-Cell simulations

This work was supported by the U.S. Department of Energy (DOE) Office of Science, LaserNetUS, Offices of High Energy Physics and Fusion Energy Sciences (FES), and used resources at NERSC under Contract No. DE-AC02-05CH11231 via the award FES-ERCAP0024250 as well as an ALCC award at OLCF (No. DE-AC05-00OR22725). S. Hakimi was supported by the U.S. DOE FES Postdoctoral Research Program administered by the Oak Ridge Institute for Science and Education (ORISE) for the DOE. ORISE is managed by Oak Ridge Associated Universities (ORAU) under Contract No. DE-SC0014664. All opinions expressed in this paper are those of the authors and do not necessarily reflect the policies and views of DOE, ORAU, or ORISE. WarpX was supported by the Exascale Computing Project (No.17-SC-20-SC), a collaborative effort of two U.S. DOE organizations (Office of Science and the National Nuclear Security Administration).

## I. INTRODUCTION

Laser-driven ion sources [1] hold unique properties such as small source size, short pulse duration, high particle number and low emittance. They are therefore of interest for a variety of applications including discovery science studies in high energy density science and warm dense matter research [2], material science, e.g., for semiconductor manufacturing and

color center formation to investigate quantum information applications [3], radiography, e.g., for imaging the electromagnetic fields generated in plasmas with high temporal and spatial resolution [4], and radiobiological studies [5]. Ion beams are well suited for radiobiological studies as a result of their localized energy deposition in the characteristic Bragg peak. Additionally, laser-driven ion beams uniquely feature ultra-high instantaneous dose rates, where the FLASH radiotherapy effect [6] can induce differential normal tissue sparing without significant changes to the therapeutic tumor response.

Laser-driven protons generated by the BELLA PW laser [7] have recently been used to conduct radiobiological studies at ultra-high instantaneous dose rates [5]. Protons were accelerated at the interaction point 1 of the BELLA Center, where an  $f/65$  off-axis parabolic (OAP) mirror provides a maximum on-target peak intensity of  $I = 1.2 \times 10^{19} \text{ W/cm}^2$ . A compact, tunable, active plasma lens beamline was used to transport accelerated protons in the range of 2–7 MeV to a custom-built cell culture chamber to irradiate mono-layer normal and tumor cell samples *in vitro*. The study successfully demonstrated that there is in fact a differential sparing of healthy cells when laser-driven proton beams are used for cell irradiation [5].

In order to realize the potential of laser-driven ion beams for applications, improvements in their parameters, e.g., maximum energy, divergence, and number of accelerated ions, are required as well as a stable and reliable operation at high repetition rates. For example, the next step for radiobiological studies is advancing to *in vivo* studies where proton energies of several 10s of MeV are required in order to perform volumetric irradiation of several mm diameter tumors in small animals [8]. Ultimately, proton energies ranging from 70 to 250 MeV are required for laser-driven proton therapy in humans.

The basic laser-driven ion acceleration mechanisms include Target Normal Sheath Acceleration (TNSA) [9], Coulomb Explosion (CE) [10], Radiation Pressure Acceleration (RPA) [11], Shock Acceleration (SA) [12] and Magnetic Vortex Acceleration (MVA) [13]. TNSA poses less stringent requirements to laser and target conditions than the other mechanisms and has been most widely studied in experiments. Advanced mechanisms [14], such as RPA and MVA, require ultra-high intensity and ultra-high contrast pulses and therefore have proven to be more challenging to reach in experiments. These regimes promise better energy scaling and quality beams. Further experiments should be conducted targeting these regimes in order to realize ion beam parameters required for the foreseen applications. In this proceeding, we describe a new high intensity beamline, named interaction point 2 (iP2), that has recently been constructed and commissioned at the BELLA Center [15]. This beamline has a short focal length focusing optic and a new target chamber, dedicated to experiments at ultra-high intensity and temporal contrast, such as laser-solid interactions in novel regimes.

## II. NEW iP2 BEAMLINE AT BELLA PW FACILITY

The new iP2 beamline is an extension to the existing BELLA PW laser with an on-demand double plasma mirror

(DPM) setup option in the upstream target chamber (interaction point 1) to clean the laser pulse from preceding prepulses and pedestals. After reflecting off the two plasma mirrors, the diverging beam is routed towards a long focal length OAP, which re-collimates the beam and sends it to the iP2 chamber, where the beam is focused to a spot size of a few microns with the short focal length ( $f/2.5$ ) OAP. To date, the iP2 beamline has been commissioned for operation with up to 17 J of laser energy. The intensity profile in the iP2 focus is measured at low power, where the fully amplified laser pulse is attenuated by reflecting off of two uncoated wedges and a neutral density foil (optical density of  $\sim 6$ ) before compression. Focal spot measurements, conducted during the commissioning experiments at 17 J, demonstrate a beam profile with a FWHM of  $2.7 \mu\text{m}$  in both the horizontal and vertical directions, as shown in Fig. 1. The angular fluctuation was measured to be 1.3 and  $2 \mu\text{rad}$  corresponding to a pointing stability of 0.64 and  $1 \mu\text{m}$  in the horizontal and vertical directions at the focal plane. Based on measurements of the focal spot size and wavefront (not shown here) at 17 J, we expect a peak intensity of  $>5 \times 10^{21} \text{ W/cm}^2$  at the full 40 J pulse energy. After the addition of an on-demand double plasma mirror (scheduled for this year), we anticipate an ultra-high temporal contrast ratio of  $<10^{-14}$ .

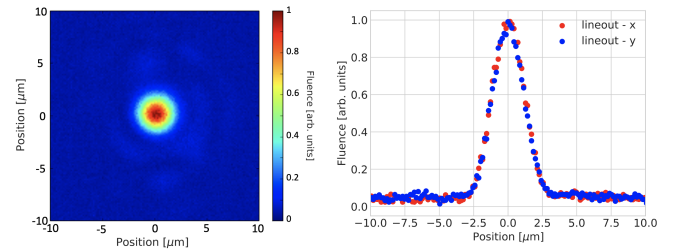


Fig. 1. iP2 focal spot measurement (without the DPM). (Left) iP2 mode measured during the commissioning experiments at 17 J of laser energy, normalized to the peak value. (Right) Horizontal, in red, and vertical, in blue, lineouts of the mode with a measured FWHM of  $2.7 \mu\text{m}$  in both directions.

The iP2 chamber can be configured with normal and oblique incidence angles on target [15]. Before entering the iP2 chamber, the laser pulse properties (spectral, spatial and temporal) can be measured at full power using a high power diagnostic suite. The thoroughly characterized laser pulses are delivered to the target with flexible experimental arrangements and diagnostics. The main diagnostics for accelerated ion beams at iP2 are a Thomson parabola spectrometer (TPS) paired with a microchannel plate (MCP) detector for the spectral characterization of the accelerated ion species, and radiochromic film (RCF) stacks for measurements of the absolute proton number and the angular proton emission distribution.

The recent commissioning experiments were conducted with an oblique incidence angle of  $\theta = 31^\circ$  onto several types of targets. During these experiments, the laser energy was increased from 4 to 17 J while the accelerated ion beams, the level of generated gamma and neutron radiation [16] and back reflections to the laser chain were closely monitored. The iP2

commissioning experiments at 17 J generated high charge, up to 40 MeV proton beams. Figure 2 shows an example image of the observed ion traces from an interaction with 13  $\mu\text{m}$  Kapton foil, with analytical solutions for different ion species overlaid. The proton trace up to 40 MeV is visible and distinguishable from the heavier ion traces. Proton beam profiles for different energy classes at specific layers in the RCF stack are shown in Fig. 2 as well. The deposited dose in Gy is shown with the color scale. The RCF stacks were located 5 cm from the interaction point and positioned to intersect the proton beams in the middle to allow an open path for the transmitted laser light.

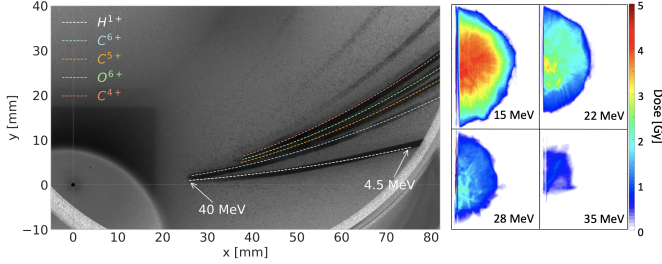


Fig. 2. TPS and RCF results from two separate shots on 13  $\mu\text{m}$  Kapton foil. (Left) Observed ion traces with the analytical solutions overlaid. The proton trace up to 40 MeV is visible and distinguishable from heavier ion traces. (Right) Proton beam (half) profile on different layers in the RCF stack. The deposited dose in Gy is shown with the color scale. We observed proton signal up to the 24th film layer, corresponding to a cutoff energy of 39 MeV.

At 17 J of pulse energy, significant back reflections were observed that ultimately led to damages in the booster amplifier of the BELLA PW [7]. Plasma mirrors are effective tools to block back reflections; therefore, the commissioning of the iP2 beamline at full power is planned in the near future, after the installation of the on-demand DPM on the beamline. We anticipate at least 24 J of pulse energy on target when using the DPM. Additional methods to avoid laser damage from back reflections will also be implemented to eventually allow for 40 J shots on targets in iP2.

The iP2 beamline operating at full energy will provide the necessary ultra-high intensity and temporal contrast to systematically study advanced ion acceleration mechanisms and explore their applications at high repetition rates. Furthermore, iP2 will operate in the intensity regime where multiple mechanisms play a role in the acceleration process and the scaling laws intersect; therefore, transitions from one regime dominating the acceleration to another can be investigated at iP2. Scaling laws and 3D simulations of the MVA regime suggest generation of protons with energies above 100 MeV near iP2's maximum intensity [15], which would be suitable for medical studies as they can penetrate a few centimeters deep into tissue [17].

Planned upcoming experiments at iP2 will study the advanced ion acceleration mechanisms and radiobiological applications with the FLASH effect. The previous radiobiological studies at the BELLA Center irradiated mono-layer cell samples [5]. The iP2 beamline boosts the TNSA proton energies

to around 40 MeV, as demonstrated by the commissioning results, allowing for small animal, *in vivo* studies with a high dose per shot. A flexible proton transport beamline using permanent magnet quadrupoles [18] has been designed to transport 10 – 30 MeV proton beams to the irradiation site and to provide a homogeneous lateral and depth dose profile to a biological sample.

Another planned experiment will explore the novel regime of Magnetic Vortex Acceleration (MVA) [13], [15]. MVA differs from the other mechanisms mainly due to the fact that the laser pulse propagates in near critical density (NCD) targets of 10s of  $\mu\text{m}$  thickness and generates an azimuthal magnetic field in the self-generated density channel. When the laser pulse and the magnetic field behind it leave the target from its rear side, the magnetic field expands into the vacuum and forms a toroidal vortex in 3D. The magnetic pressure displaces the electron component of the plasma relative to the ions and a quasistatic electric field, on the order of 10s of TV/m, is formed. This field accelerates and collimates the ions from the filament. Collimated ion beams from MVA would also facilitate subsequent capture and transport for future radiobiological studies.

### III. SIMULATIONS OF THE MAGNETIC VORTEX ACCELERATION REGIME

In order to prepare for the upcoming experiments to investigate the MVA regime, a series of 3D Particle-in-Cell (PIC) simulations, using the WarpX code [19], were performed to study the optimal performance and robustness of MVA with iP2 beamline parameters and as close to the experimental conditions as possible. In a PW-class laser, a nanosecond pedestal and short prepulses result in the formation of a preplasma on the front and rear sides of the target. We studied the acceleration performance of MVA under varied density ramps to model pre-expanded target profiles. This is of interest for the case of non-ideal laser contrast cleaning as well as when the DPM is not used. In the MVA regime, the variation of the plasma density in the rear side of the target is closely related to the magnetic field expansion, which affects the acceleration process. The direction and collimation of ion beams in the case of an off-normal angle of incidence were also studied to model experimental constraints, where back reflections into the laser chain need to be avoided for laser safety. Simulations were performed with pure hydrogen and composite targets to investigate multi-species effects.

Optimization conditions for MVA require matching the laser focal spot size to the diameter of the self-generated channel as well as matching the target thickness and density to the laser depletion length [20]. In principle, the target parameters can be chosen to maximize the ion energy for a set of laser parameters [21]. Since the focal spot size of iP2 is fixed by the f/2.5 focusing optic, we match the channel diameter to the focal spot size by adjusting the plasma density. A series of 2D scans were performed to optimize the target parameters, resulting in a density of  $n_e = 2n_{cr}$  and a thickness

of  $L_{\text{ch}} = 28 \mu\text{m}$  for the 0.5 PW (iP2 with DPM setup) laser pulse focused to a  $2.5 \mu\text{m}$  focal spot.

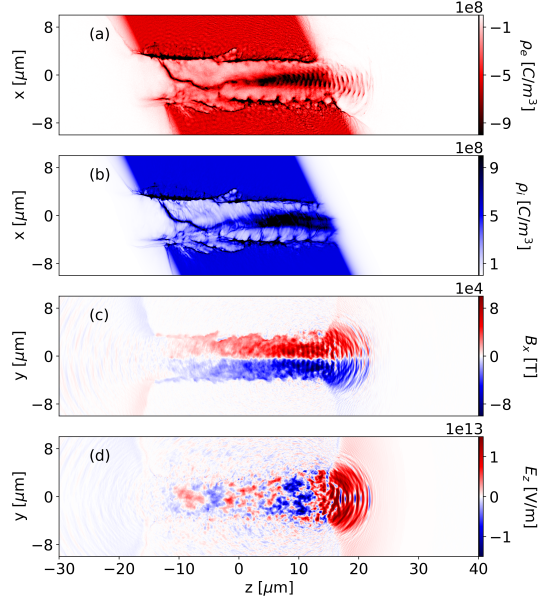


Fig. 3. Density and field evolution from a 3D simulation of the MVA regime with a composite target, target tilt of  $25^\circ$ , and a preplasma scale length of  $1 \mu\text{m}$ . (a) Electron density, (b) ion density including protons and  $\text{C}^{6+}$  ions, (c) azimuthal magnetic field as shown as  $B_x$  in the  $yz$  plane, and (d)  $E_z$  field in the horizontal slice at  $t = 96$  fs, the onset of the acceleration stage, are shown.

The 3D simulations were performed with realistic iP2 laser parameters in focus, assuming 75 % and 50 % energy confinement in time and space respectively. The laser is linearly polarized in  $x$  (p-polarized) with both a transverse and longitudinal Gaussian profile and propagates along the  $z$ -axis. The laser wavelength is  $815 \text{ nm}$  and the pulse duration is  $35 \text{ fs}$ . The laser pulse is tightly focused  $2 \mu\text{m}$  behind the target front surface to a FWHM of  $2.5 \mu\text{m}$ . The laser intensity is  $6.05 \times 10^{21} \text{ W/cm}^2$  corresponding to an  $a_0 = 55$  without contrast cleaning and  $3.63 \times 10^{21} \text{ W/cm}^2$  corresponding to an  $a_0 = 42$  with contrast cleaning, if the DPM setup is used. The optimized target conditions of  $n_e = 2n_{\text{cr}}$  and  $L_{\text{ch}} = 28 \mu\text{m}$  are used for the 3D simulations. The simulation setup is discussed in more detail in [15]. Simulations were performed with  $\theta = 0^\circ$  and  $25^\circ$  angle of incidence. Exponential density ramps with  $\sigma = 1-5 \mu\text{m}$  scale lengths were added to the target symmetrically at the front and rear sides to study the effects of preplasma and target expansion. Simulations were performed with two types of targets: pre-ionized pure hydrogen and the atomic composition of Liquid Crystal Targets 8CB (4-octyl-4'-cyanobiphenyl)  $\text{C}_{21}\text{H}_{25}\text{N}$  (LCT), which were simplified to  $\text{C}_{22}\text{H}_{25}$ . A controlled laser prepulse can be used in order to pre-expand LCT to  $2n_{\text{cr}}$ .

The electron and ion density distributions from one of the composite target simulations with an off-normal angle of incidence ( $a_0 = 55$ ,  $\theta = 25^\circ$ ,  $\sigma = 1 \mu\text{m}$ ) at  $t = 96$  fs are shown in Fig. 3 (a and b). Here, referenced times are relative to the laser focus,  $2 \mu\text{m}$  behind the target front surface. In

general, the electron and ion channels are robustly generated in simulations with tilted targets. The electron current inside the channel generates a strong azimuthal magnetic field on the order of  $0.1 \text{ MT}$ , shown in Fig. 3 (c), which is expected for a PW laser pulse. The azimuthal magnetic field is plotted as  $B_x$  in the  $yz$  plane to visualize it separately from the magnetic field of the laser in the  $y$ -direction. The expansion of the magnetic field as it leaves the target displaces surface electrons, resulting in a strong longitudinal electric field at the rear surface of the target. This field is on the order of  $10\text{s of TV/m}$ , shown in Fig. 3 (d), and will accelerate ions from the central ion filament inside the channel. For this simulation, this time corresponds to the onset of magnetic field expansion at the target rear. Simulations also show the generation of high energy electrons, a signature of the MVA mechanism. The maximum electron energy is reached at  $t = 76$  fs, approximately when the laser pulse exits the target.

From the initial  $40 \text{ J}$  of the laser energy in this simulation,  $0.64 \text{ J}$  is transferred to the combined proton and  $\text{C}^{6+}$  beams translating to  $1.6 \%$  conversion efficiency. From this  $0.64 \text{ J}$ ,  $70.56 \%$ ,  $14.65 \%$ ,  $4.45 \%$ , and  $0.27 \%$  are transferred to protons with  $E < 25$ ,  $25 < E < 50$ ,  $50 < E < 75$ , and  $75 < E \text{ MeV}$  respectively and the remaining  $10.07 \%$  is transferred to the  $\text{C}^{6+}$  beam. The direction of acceleration in the tilted target geometry is normal to the target rear as demonstrated in Fig. 4 for this simulation, where proton and  $\text{C}^{6+}$  density distributions are shown at  $t = 146$  fs. The spatial distribution of accelerated proton and  $\text{C}^{6+}$  beams, integrated for positions  $> 20 \mu\text{m}$  are also shown at several energy levels. The center of the beams are offset in the  $x$ -direction from the laser axis indicating the direction of acceleration to be nearly normal to the target rear.

Proton and  $\text{C}^{6+}$  energies of up to  $125 \text{ MeV}$  and  $37 \text{ MeV/n}$ , respectively, were observed in these simulations. The acceleration stage is identifiable with a steep rise in ion energy that lasts for  $100-200 \text{ fs}$  from when the laser pulse exits the target rear until energy is converged. The generated ion beams have a low divergence in the range of  $7-15^\circ$  for  $E > 0.4E_{i,\text{max}}$ . Divergence is defined as  $2\Delta\theta = 2\sqrt{\langle(\theta^2)\rangle - \langle\theta\rangle^2}$  where  $\langle\rangle$  is the average of the angular distribution in each energy bin and  $\theta$  is defined as the angle to the laser axis. This narrow divergence results from the transverse electric field generated at the target rear side [15], [20].

#### IV. CONCLUSIONS

A new platform for experimental investigation of ultra-high intensity laser-plasma interactions, iP2, has been constructed and commissioned recently. The iP2 beamline is an addition to the BELLA PW facility, operating at  $1 \text{ Hz}$  repetition rate, with a short focal length focusing optic, a new experimental target chamber and dedicated diagnostics. An on-demand DPM will be installed on the beamline to mitigate back reflection issues and produce an ultra-high contrast pulse. The recent commissioning of this beamline up to  $17 \text{ J}$  of laser energy has demonstrated a focused beam of  $2.7 \mu\text{m}$  in both horizontal and vertical directions. The commissioning



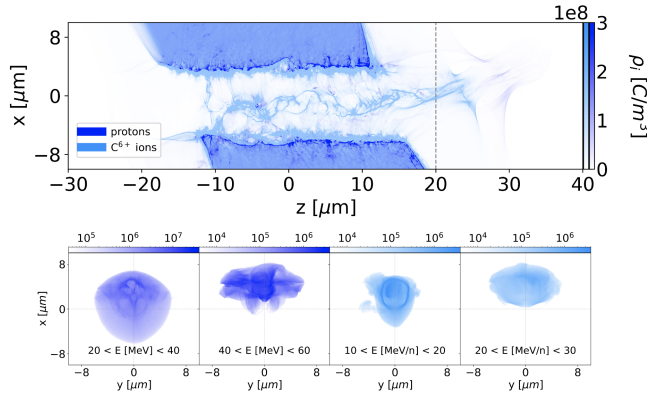


Fig. 4. 3D simulation results. (Top) Proton and  $C^{6+}$  density distributions at  $t = 146$  fs, showing acceleration in the normal direction to the target. (Bottom) The spatial distribution of accelerated proton and  $C^{6+}$  beams in the  $xy$  plane, integrated for positions  $>20$   $\mu\text{m}$ , shown for different energy levels. The center of the beams are offset from the laser axis in the  $x$  direction toward the target normal direction.

experiments in the TNSA regime have already produced high charge, up to 40 MeV proton beams. Future experiments will study radiobiological applications of TNSA produced proton beams and investigate advanced ion acceleration regimes. An experimental campaign is planned to study the novel regime of MVA with NCD targets in extensive detail. A comprehensive study of this regime with 3D PIC simulations, using iP2 parameters, was done to inform the planning and preparation for this campaign.

#### ACKNOWLEDGMENT

We gratefully acknowledge technical support from Zachary Eisentraut, Mark Kirkpatrick, Tyler Sipla, Jonathan Bradford, Haris Muratagic, Gregory Scharfstein, Nathan Ybarrolaza, Greg Mannino, Paul Centeno, Derrick McGrew, Thorsten Stezelberger, Arturo Magana, Joe Riley, Zachary Harvey and the Radiation Protection Group of LBNL. We thank all the contributors from the WarpX community who participated in code improvement.

#### REFERENCES

- [1] A. Macchi, M. Borghesi, M. Passoni, "Ion acceleration by superintense laser-plasma interaction," *Reviews of Modern Physics*, vol. 85, pp. 751, 2013. H. Daido, M. Nishiuchi, A. S. Pirozhkov, "Review of laser-driven ion sources and their applications," *Reports on progress in physics*, vol. 75, pp. 056401, 2012.
- [2] P. K. Patel, A. J. Mackinnon, M. H. Key, T. E. Cowan, M. E. Foord, M. Allen, "Isochoric heating of solid-density matter with an ultrafast proton beam," *Physical review letters*, vol. 91, pp. 125004, 2003.
- [3] R. E. Russel, A. Persaud, C. Christian, E. S. Bernard, E. M. Chan, A. A. Bettiol, "Direct formation of nitrogen-vacancy centers in nitrogen doped diamond along the trajectories of swift heavy ions," *Applied Physics Letters*, vol. 118, pp. 084002, 2021. W. Redjem, A. J. Amsellem, F. I. Allen, G. Benndorf, J. Bin, S. Bulanov, "Defect engineering of silicon with ion pulses from laser acceleration," *arXiv:2203.13781*, 2022.
- [4] M. Borghesi, J. Fuchs, S. V. Bulanov, A. J. Mackinnon, P. K. Patel, M. Roth, "Fast ion generation by high-intensity laser irradiation of solid targets and applications," *Fusion science and technology*, vol. 49, pp. 412–439, 2006.
- [5] J. Bin, L. Obst-Huebl, J.-H. Mao, K. Nakamura, L. D. Geuling, H. Chang, "A new platform for ultra-high dose rate radiobiological research using the BELLA PW laser proton beamline," *Scientific reports*, vol. 12, pp. 1484, 2022. S. Boucher, E. Esarey, C. Geddes, C. Johnstone, S. Kutsaev, B. W. Loo, "Transformative technology for flash radiation therapy: A snowmass 2021 white paper," *arXiv:2203.11047*, 2022.
- [6] A. A. Friedl, K. M. Prise, K. T. Butterworth, P. Montay-Gruel, V. Favaudon, "Radiobiology of the FLASH effect," *Medical Physics*, vol. 49, pp. 1993–2013, 2022.
- [7] K. Nakamura, H.-S. Mao, A. J. Gonsalves, H. Vincenti, D. Mittelberger, J. Daniels, "Diagnostics, control and performance parameters for the BELLA high repetition rate petawatt class laser," *IEEE Journal of Quantum Electronics*, vol. 53, pp. 1–21, 2017.
- [8] F. Kroll, "Forschungsteam schafft Meilenstein bei der Bestrahlung mit Protonen," *TumorDiagn u Ther*, vol. 43, 2022. K. Zeil, "High energy proton acceleration at DRACOPW and radio-biological applications," in this Proceedings – submitted.
- [9] S. C. Wilks, A. B. Langdon, T. E. Cowan, M. Roth, M. Singh, S. Hatchett, "Energetic proton generation in ultra-intense laser–solid interactions," *Physics of plasmas*, vol. 8, pp. 542–549, 2001.
- [10] I. Last, I. Schek, J. Jortner, "Energetics and dynamics of Coulomb explosion of highly charged clusters," *The Journal of chemical physics*, vol. 107, pp. 6685–6692, 1997. T. Ditmire, J. W. G. Tisch, E. Springate, M. B. Mason, N. Hay, R. A. Smith, "High-energy ions produced in explosions of superheated atomic clusters," *Nature*, vol. 386, pp. 54–56, 1997.
- [11] T. Esirkepov, M. Borghesi, S. V. Bulanov, G. Mourou, T. Tajima, "Highly efficient relativistic-ion generation in the laser-piston regime," *Physical review letters*, vol. 92, pp. 175003, 2004.
- [12] L. O. Silva, M. Marti, J. R. Davies, R. A. Fonseca, C. Ren, F. S. Tsung, "Proton shock acceleration in laser-plasma interactions," *Physical Review Letters*, vol. 92, pp. 015002, 2004.
- [13] A. V. Kuznetsov, T. Z. Esirkepov, F. F. Kamenets, S. V. Bulanov, "Efficiency of ion acceleration by a relativistically strong laser pulse in an underdense plasma," *Plasma Physics Reports*, vol. 27, pp. 211–220, 2001. S. V. Bulanov, D. V. Dylov, T. Z. Esirkepov, F. F. Kamenets, D. V. Sokolov, "Ion acceleration in a dipole vortex in a laser plasma corona," *Plasma physics reports*, vol. 31, pp. 369–381, 2005.
- [14] S. S. Bulanov, E. Esarey, C. B. Schroeder, S. V. Bulanov, T. Z. Esirkepov, M. Kando, "Radiation pressure acceleration: The factors limiting maximum attainable ion energy," vol. 23, pp. 056703, 2016. S. S. Bulanov, "Advanced Ion Acceleration Mechanisms," in this Proceedings – submitted.
- [15] S. Hakimi, L. Obst-Huebl, A. Huebl, K. Nakamura, S. S. Bulanov, S. Steinke, "Laser–solid interaction studies enabled by the new capabilities of the iP2 BELLA PW beamline," *Physics of Plasmas*, vol. 29, pp. 083102, 2022.
- [16] C. Toth, A. J. Gonsalves, K. Nakamura, L. Obst-Huebl, M. Turner, A. Picksley, "Radiation and Laser Safety Implementations for Safe and Efficient User Experiments at the Upgraded BELLA PW iP2 & 2BL Beamlines," in this Proceedings – submitted.
- [17] F. Albert, M. E. Couprie, A. Debus, M. C. Downer, J. Fraue, A. Flacco, "2020 roadmap on plasma accelerators," *New Journal of Physics*, vol. 23, pp. 031101, 2021.
- [18] J. T. De Chant, K. Nakamura, Q. Ji, L. Obst-Huebl, S. Steinke, S. Barber, "Design Optimization of Permanent-Magnet Based Compact Transport Systems for Laser-Driven Proton Beams," in this Proceedings – submitted.
- [19] L. Fedeli, A. Huebl, F. Boillod-Cerneux, T. Clark, K. Gott, C. Hillairet, "Pushing the Frontier in the Design of Laser-Based Electron Accelerators with Groundbreaking Mesh-Refined Particle-In-Cell Simulations on Exascale-Class Supercomputers," *SC22: International Conference for High Performance Computing, Networking, Storage and Analysis (SC)*. ISSN:2167-4337, pp. 25–36, 2022.
- [20] J. Park, S. S. Bulanov, J. Bin, Q. Ji, S. Steinke, J.-L. Vay, "Ion acceleration in laser generated megatesla magnetic vortex," *Physics of Plasmas*, vol. 26, pp. 103108, 2019.
- [21] S. S. Bulanov, V. Y. Bychenkov, V. Chvykov, G. Kalinchenko, D. W. Litzenberg, T. Matsuoka, "Generation of GeV protons from 1 PW laser interaction with near critical density targets," *Physics of plasmas*, vol. 17, pp. 043105, 2010.